SUPPLEMENTAL INFORMATION

Structural basis for non-canonical kinase-substrate recognition of cofilin/ADF proteins by LIM kinases

Authors

Stephanie Hamill[1], Hua Jane Lou[1], Benjamin E. Turk[1,3] and Titus J. Boggon*[1,2,3]

Affiliation

Departments of [1]Pharmacology and [2]Molecular Biophysics and Biochemistry, and the [3]Yale Cancer Center, Yale University School of Medicine, New Haven, CT 06520

***To who correspondence should be addressed**

titus.boggon@yale.edu

SUPPLEMENTAL FIGURES

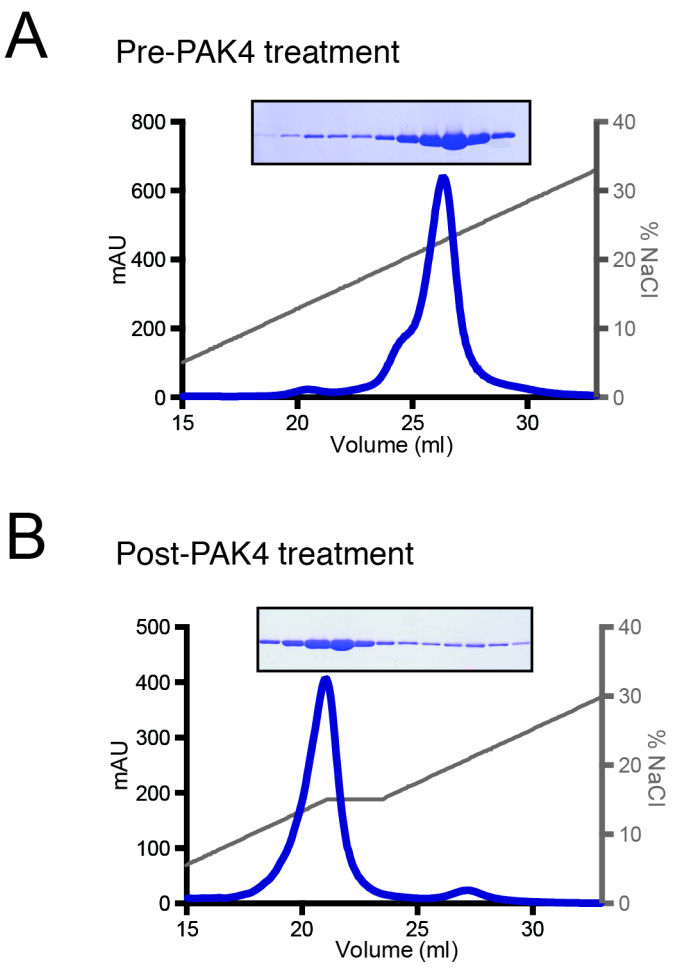

Figure S1. Related to Figure 1. Purification of $LIMK1_{CAT}$. A) Cationic exchange chromatography for $LIMK1_{CAT}^{D460N}$ prior to treatment with PAK4. **B)** Cationic exchange chromatography for $pLIMK1_{CAT}^{D460N}$ following treatment with PAK4. PAK4-treated $pLIMK1_{CAT}^{D460N}$ elutes at a lower salt concentration than untreated $LIMK1_{CAT}^{D460N}$.

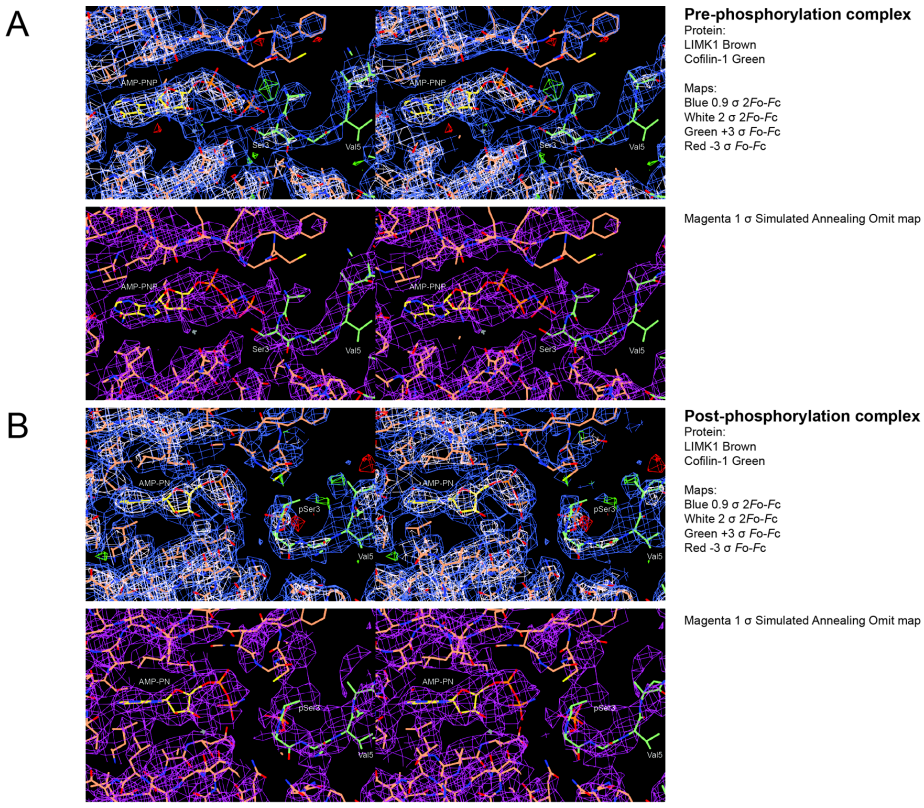

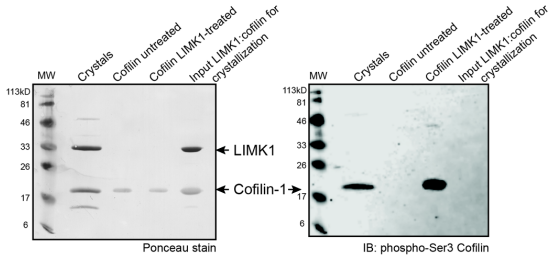

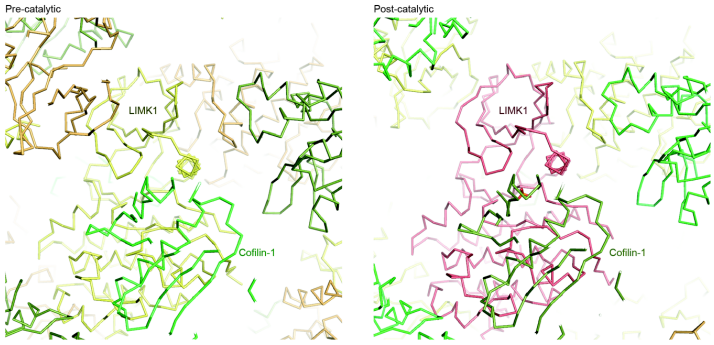

Figure S2. Related to Figure 2. Features of the pLIMK1$_{CAT}^{D460N}$:cofilin-1 co-crystal structure. A, B) Stereoviews of electron density for A) pre-catalytic and B) post-catalytic

complexes found in the asymmetric unit. Stick representation shown for cofilin-1 (green), LIMK1 (brown) and nucleotide. Top panels show $2F_{obs}$-F_{calc} map at 2 σ (white) and 0.9 σ (blue) and F_{obs}-F_{calc} map at +3 σ (green) and -3 σ (red), bottom panels show simulated annealing omit map at 1.0 σ (magenta). **C)** Western blot analysis of pLIMK1$_{CAT}^{D460N}$:cofilin-1 co-crystals. LIMK1:cofilin-1 co-crystals were carefully washed 3 times. Analysis was conducted by SDS-PAGE and immunoblotting with anti-phospho-Ser3 Cofilin antibody (right), and by Ponceau staining (left). Lanes indicated: LIMK1:cofilin-1 co-crystals (Crystals), purified cofilin-1 (Cofilin untreated), purified cofilin-1 *in vitro* phosphorylated by LIMK1$_{CAT}$ (Cofilin LIMK1-treated), protein sample used to set up co-crystallization trials (Input LIMK1:cofilin for crystallization). **D)** Symmetry-related crystal contacts for LIMK1:cofilin-1 co-crystal structure. Pre-catalytic (left) complex LIMK1 is shown in yellow and cofilin-1 is in green; post-catalytic (right) complex shows LIMK1 in magenta and cofilin-1 in dark green.

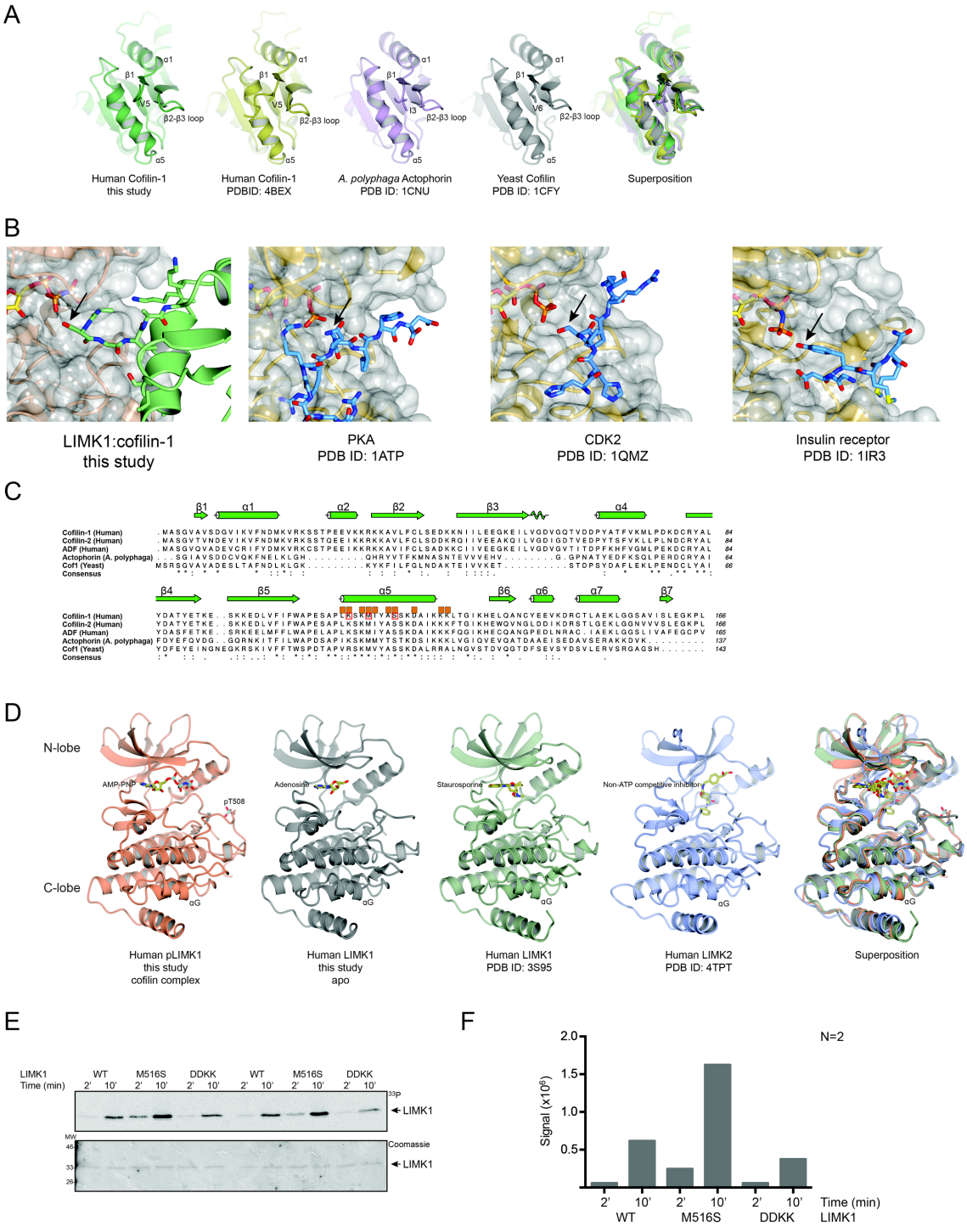

Figure S3. Related to Figure 3. Analysis of the pLIMK1$_{CAT}^{D460N}$:cofilin-1 co-crystal structure. A) Superposition of cofilin crystal structures. Human Cofilin-1 from

pLIMK1$_{CAT}^{D460N}$:cofilin-1 co-crystal structure (green, this study), human cofilin-1 (yellow, PDB ID: 4BEX (Klejnot et al., 2013)), *A. polyphaga* Actophorin (purple, PDB ID: 1CNU (Blanchoin and Pollard, 1998)), yeast cofilin-1 (grey, PDB ID: 1CFY, (Fedorov et al., 1997)). The residue positioned in between helix α5 and the β2-β3 loop is drawn in stick format (Val5 in human cofilin-1). **B)** Comparison of kinase-substrate pairs. From left to right: pLIMK1$_{CAT}^{D460N}$:cofilin-1. Cyclic AMP-dependent protein kinase PKA in complex with a non-phosphorylatable substrate peptide (PDB ID: 1ATP) (Zheng et al., 1993). Cyclin dependent kinase 2 (CDK2) in complex with a peptide substrate (PDB ID: 1QMZ) (Brown et al., 1999). Insulin receptor in complex with a peptide substrate (PDB ID: 1IR3) (Hubbard, 1997). Arrow indicates phosphoacceptor residue. Kinase shown with a transparent surface, and substrate in stick format. ATP or ATP analogue shown in stick format. **C)** Sequence alignment. Alignment shown of human cofilin-1 (Uniprot ID: P23528), human cofilin-2 (Uniprot ID: Q9Y281), human actin depolymerizing factor (ADF) (Uniprot ID: P60981), *Acanthamoeba polyphaga* Actophorin (Uniprot ID: P37167)(PDB ID: 1CNU) and *Saccharomyces cerevisiae* cofilin-1 (Uniprot ID: Q03048)(PDB ID: 1CFY). Sequence alignment conducted using Clustal Omega (Sievers et al., 2011). Secondary structure features indicated and nomenclature based on (Klejnot et al., 2013). Orange boxes indicate residues that interact with LIMK1 by PDBSum (Laskowski, 2009). Residues that are mutated in this study are boxed in red. **D)** Superposition of LIM kinase crystal structures. Human phospho-LIMK1 (pT508) (brown, this study), human unphosphorylated LIMK1 (grey, this study), human LIMK1 (green, PDB ID: 3S95, unpublished), human LIMK2 (blue, PDB ID: 4TPT, (Goodwin et al., 2015)). Bound nucleotide or inhibitor shown. Structures superposed on the C-lobe of LIMK1 using CCP4mg (McNicholas et al., 2011). **E)** *In vitro* kinase assay. Autoradiography showing autophosphorylation of LIMK1$_{CAT}$ (top). Mutants are indicated. Loading indicated by Coomassie stained SDS-PAGE (bottom). Two time points shown. **F)** Quantitation of kinase assay. Average of 2 experiments shown. LIMK1$_{CAT}^{M516S}$ (M516S) and LIMK1$_{CAT}^{DDKK}$ (DD549/551KK) mutants are both active kinases.

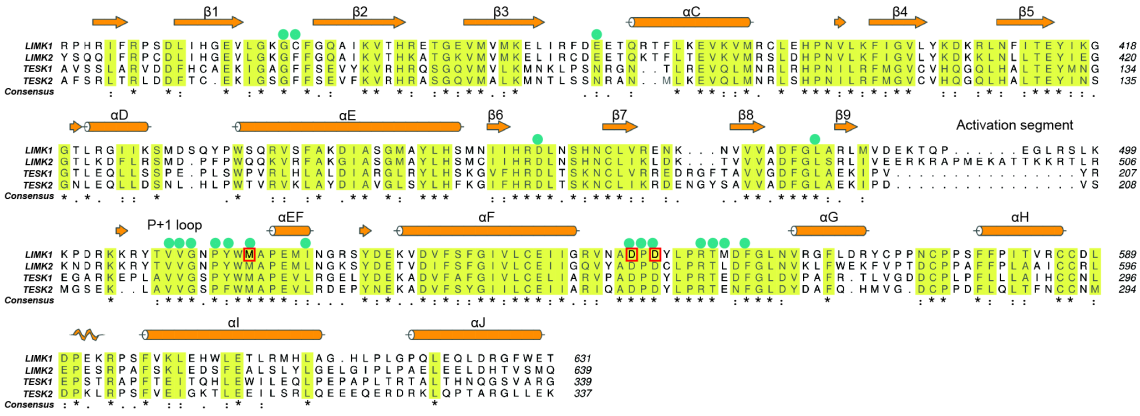

Figure S4. Related to Figure 5. Sequence alignment of human LIM kinases. Sequence alignment of the catalytic domains of human LIMK1 (Uniprot ID: P53667), LIMK2 (Uniprot ID: P53671), TESK1 (Uniprot ID: Q15569) and TESK2 (Uniprot ID: Q96S53) conducted by Clustal Omega (Sievers et al., 2011). Residues highlighted in yellow are highly conserved. Secondary structure features indicated. Residues mutated in this study are indicated with red boxes. Blue circles indicate residues that interact with Cofilin-1 in both heterodimers by PDBSum (Laskowski, 2009). Consensus indicated: complete conservation (*), strong similarity (:), weak similarity (.).

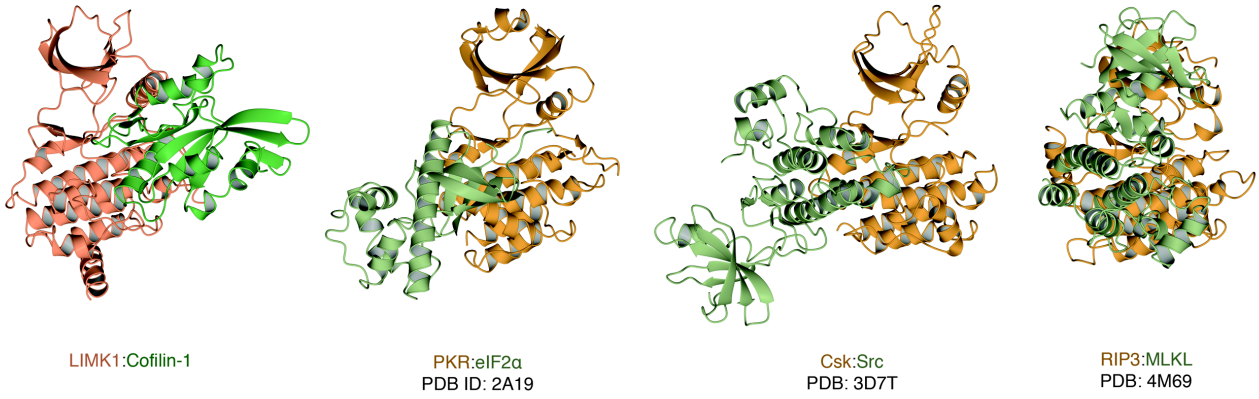

Figure S5. Related to Figure 6. Comparison of co-crystal structures of protein kinases in complex with folded protein substrates. pLIMK1$_{CAT}^{D460N}$:cofilin-1 co-crystal shown on left. PKR-eIF2α (PDB ID: 2A19) (Dar et al., 2005), CSK-Src (PDB ID: 3D7T) (Levinson et al., 2008) and RIP3-MLKL (PDB ID: 4M69) (Xie et al., 2013) shown. Catalytic kinase domains shown in brown. Substrates shown in green. Structures shown in same orientation of the kinase domain based on superposition on the LIMK1 kinase C-lobe using CCP4mg (McNicholas et al., 2011).

SUPPLEMENTAL EXPERIMENTAL PROCEDURES

Protein expression and purification

For co-crystallization of pLIMK1$_{CAT}^{D460N}$ with cofilin-1

Optimized cDNA (GenScript) for human LIMK1 (UniProt ID: P53667) kinase domain (LIMK1$_{CAT}$: residues 329-638) containing point mutation D460N (LIMK1$_{CAT}^{D460N}$) was subcloned into a GST-tagged transfer vector derived from pFastBac Htb (Invitrogen) using BamHI and NotI restriction enzyme sites. Recombinant baculovirus was generated using the Bac-to-Bac Baculovirus expression system (Invitrogen) and the kinase domain was expressed as a Glutathione S-transferase (GST) fusion protein with a Tobacco Etch Virus protease (TEV) site located between GST and LIMK1$_{CAT}^{D460N}$. *Spodoptera frugiperda* (Sf9) cells (Gibco) infected with the recombinant baculovirus were grown in shaker flasks and SF900 II media (Gibco) and harvested 72 hours after infection. Cells were harvested and resuspended in 20 ml lysis buffer (50 mM Tris, pH 7.4, 150 mM NaCl, 1 mM dithiothreitol [DTT], 5% glycerol, protease inhibitor cocktail (Roche)) and lysed by sonication. Following cell lysis, clarified supernatant is applied to 2 ml Glutathione Sepharose 4B resin (GE Healthcare). Overnight treatment with TEV protease at 4°C cleaved GST and LIMK1$_{CAT}$, and the eluate (containing LIMK1$_{CAT}^{D460N}$) was applied to a 1 ml Resource S column (GE Healthcare) equilibrated with 50 mM Tris, pH 7.4, 50 mM NaCl, 1 mM DTT, 5% glycerol. LIMK1$_{CAT}^{D460N}$ was eluted by increasing NaCl concentration, concentrated and then purified by size exclusion chromatography on a Superdex 200 10/300 GL column (GE Healthcare). LIMK1$_{CAT}^{D460N}$ eluted as a monodisperse peak.

To phosphorylate LIMK1$_{CAT}^{D460N}$, purified LIMK1$_{CAT}^{D460N}$ was treated with recombinant PAK4 catalytic domain, purified as described below, in the presence of 50 mM ATP, 5 mM $MgCl_2$ and 1 mM $MnCl_2$ at a ratio of approximately 1:0.5, LIMK1:PAK4. The mixture was incubated overnight at 4°C to allow PAK4 to phosphorylate LIMK1$_{CAT}^{D460N}$. Limited proteolysis followed by

mass spectrometry confirmed a single phosphorylation event on Thr508; phosphorylation of this residue in the LIMK1 activation loop is associated with kinase activation. Phospho-LIMK1$_{CAT}^{D460N}$ (pLIMK1$_{CAT}^{D460N}$) was then further purified by an additional ion exchange chromatography step on a 1 ml Resource S column (GE Healthcare), and pLIMK1$_{CAT}^{D460N}$ was separated from LIMK1$_{CAT}^{D460N}$ by earlier elution on the salt gradient. pLIMK1$_{CAT}^{D460N}$ was concentrated to 10 mg/ml for use in co-crystallization trials with cofilin.

Mature full-length human cofilin-1 (UniProt ID: P23528) (Cofilin: residues 2-166) was purified from a modified pET-28a vector which has an N-terminal His$_6$-SUMO tag. To obtain a native mature N-terminus of cofilin following treatment with SUMO protease (i.e. with N-terminal residue Ala-2) cloning-site artifacts' were removed by mutagenesis (QuikChange lightning – Agilent Technologies). Cofilin protein is produced in *E. coli* BL21(DE3) cells at density OD_{600} 0.5 by overnight induction with 0.5 mM IPTG at 18°C. Cells are harvested and resuspended in 15 ml lysis buffer (50 mM Tris, pH 7.8, 150 mM NaCl, 20 mM imidazole, 1 mM DTT supplemented with protease inhibitor cocktail, lysozyme, and DNaseI). Following cell lysis by sonication, clarified supernatant is applied to 5 ml Ni^{2+}-sepharose 6 FF resin (GE Healthcare) by batch, resin is washed with lysis buffer and protein eluted with lysis buffer supplemented with 300 mM imidazole. Following overnight treatment with SUMO protease and dialysis against 1 L lysis buffer, cofilin was applied to a 1 ml Resource Q column (GE Healthcare). The flow-through (containing cofilin) was then applied to a final round of size exclusion chromatography on a HiLoad 16/60 Superdex 75 prep column (GE Healthcare) using buffer conditions containing 20 mM Tris pH 7.5, 150 mM NaCl, 1 mM DTT. Full-length cofilin eluted as a monodisperse peak.

Human TESK1 kinase domain (UniProt ID: Q15569) (TESK1$_{CAT}$: residues 47-343) was expressed in Sf9 insect cells as a GST-fusion protein in a manner similar to LIMK1$_{CAT}$. Following cell lysis, affinity purification with 0.5 ml glutathione Sepharose 4B (GE Healthcare), and affinity-

tag cleavage with recombinant TEV. TESK1 protein was further purified by size exclusion chromatography on a Superdex 200 10/300 GL column (GE Healthcare).

All point mutants are generated using QuikChange lightning mutagenesis kit (Agilent Technologies) ($LIMK1_{CAT}$: D460N, M516S, DD549/551KK; cofilin: K112D, K114D, M115A, S119M).

For crystallization of $LIMK1_{CAT}^{D460N}$

$LIMK1_{CAT}^{D460N}$ was purified as described above but was not subjected to phosphorylation by recombinant PAK4.

For kinase activity assays

For kinase assays with cofilin, wild type $LIMK_{CAT}$ was purified as described above and treated with PAK4. Activated, pT508 LIMK was separated from unphosphorylated LIMK by cationic exchange and used in phosphorylation assays with cofilin substrate. For analysis of LIMK auto-phosphorylation at T508, purified $LIMK_{CAT}$ that had not undergone recombinant PAK4-treatment was used in kinase assays.

PAK4 kinase domain

Human PAK4 (UniProt ID: O96013) kinase domain (residues 300-591) was expressed as an N-terminal hexahistidine (His_6) maltose binding protein (MBP) fusion protein in BL21(DE3) *E. coli* cells (Ha et al., 2012). Expression was identical to the previous description, but during purification all NTA-affinity chromatography steps were supplemented with 300 mM NaCl. The eluted His_6-MBP-PAK4 was not subjected to affinity tag removal by proteolysis, and a final size exclusion chromatography step on a HiLoad 16/60 Superdex 75 prep column was performed in

buffer containing 20 mM Tris pH 7.75, 250 mM NaCl, 2.5 mM DTT, and 5% glycerol. Fractions containing purified protein were pooled and flash frozen in 150 µl aliquots.

Crystallization

Crystallization of LIMK1$_{CAT}^{D460N}$

Co-crystallization trials of LIMK$_{CAT}^{D460N}$ with a synthesized peptide corresponding to residues 2 - 10 of human cofilin-2, sequence ASGVTVNDE (Tufts Core), were attempted by mixing LIMK1$_{CAT}^{D460N}$ protein (at 8 mg/ml protein concentration) with the cofilin-2 peptide at a protein:peptide ratio of 1:1.3 in the presence of 5 mM AMP-PNP and 1 mM $MgCl_2$. Crystals grew at room temperature by the sitting-vapor diffusion method against precipitant conditions containing 20-30% PEG 3350 and 200 mM potassium citrate. Crystals were further optimized by streak-seeding into fresh drops with lower precipitant concentration (18-24% PEG 3350). Single crystals of approximately ~20 x 50 x 100 µm size grew after 2 days, and were harvested and cryoprotected in 25% glycerol and flash vitrified in liquid nitrogen.

Co-crystallization of pLIMK1$_{CAT}^{D460N}$ with cofilin-1

For co-crystallization of pLIMK1$_{CAT}^{D460N}$:cofilin-1 the proteins were mixed in a 1:1.2 molar ratio (pLIMK1$_{CAT}^{D460N}$:cofilin-1). Following concentration of the mixture to ~8 mg/ml, it was supplemented with 5 mM AMP-PNP and 1 mM $MgCl_2$. Sparse matrix screening was conducted using sitting drop vapor diffusion and the Classics, PEGs and JCSG + kits (Qiagen). Initial small 'sea urchin' crystals were obtained in one drop containing 0.1 M HEPES pH 7.5 and 1.4 M tri-Sodium citrate in the Classics Suite (Qiagen). These initial conditions were repeated and screened using hanging drop vapor diffusion at room temperature, and optimal conditions obtained using precipitant in a range of 1.2-1.4 M tri-Sodium citrate, 0.1 M sodium acetate, pH 5.5. Optimal crystallization conditions included a total drop size of 2.5 µl using a 1.5:1 ratio of protein to precipitant. Sea urchin-like crystals grew within 2 days and were further optimized by

either streak- or macro-seeding into fresh drops with lower precipitant concentration (1.0 - 1.2 sodium citrate). This yielded crystals of approximately ~15 x 15 x 100 µm size which were harvested directly from drops supplemented with 15% glycerol and flash vitrified in liquid nitrogen.

Immunoblotting of pLIMK1$_{CAT}^{D460N}$:cofilin-1 crystals

Crystals were harvested ~1 week after they appeared and were washed 3 times by sequential transfer to fresh 5 µl drops containing 2 M sodium citrate and 0.1 M sodium acetate, pH 5.5. The washed crystals were then analyzed by SDS-PAGE, transferred to a nitrocellulose membrane and probed with anti-phospho-cofilin (Ser3) rabbit mAb (Cell Signaling, 1:3000 dilution) and anti-rabbit IR Dye800 antibodies. As a control, 20 µM purified cofilin was reacted with 100 nm LIMK$_{CAT}$ in the presence of 50 mM ATP, 1 mM $MgCl_2$, and reacted at 30 °C for 30 minutes. The Western blot results were evaluated using a LiCor Imaging system.

Data collection and structure determination

Data collection and structure determination for LIMK1$_{CAT}^{D460N}$

A total of 720° of data were collected from 2 separate crystals at beamline 24-ID-E at the Advanced Photon Source. The data were integrated and scaled to 2.2 Å resolution using HKL2000 (Otwinowski and Minor, 1997) and initial phases were obtained by the molecular replacement method using Phaser (McCoy, 2007). The structure of LIMK1 in complex with the ATP competitive inhibitor staurosporine (PDB ID: 3S95) was used as the search model, and yielded a solution with a final translation Z-score of 22.6. The solution contained 2 copies of LIMK1 kinase domain per asymmetric unit. Multiple rounds of refinement and model building using Phenix (Adams et al., 2010) and Coot (Emsley et al., 2010) yielded final R and R_{free} values of 20.6% and 25.2% respectively. Electron density for the adenosine of AMP-PNP was observed bound to only one copy of LIMK$_{CAT}^{D460N}$ (chain A). No electron density was observed

for the cofilin peptide in this structure. The structure is deposited in the protein data bank under accession code 5HVJ.

Data collection and structure determination for pLIMK1$_{CAT}^{D460N}$:cofilin-1

A total of 394° of data were collected in 9 sweeps from 4 crystals at beamline 24-ID-E at the Advanced Photon Source. Merged data were integrated and scaled to 3.5 Å resolution using HKL2000 (Otwinowski and Minor, 1997). Initial phasing was obtained by the molecular replacement method implemented in the program Phaser (McCoy, 2007). Two search models were used, our 2.2 Å kinase domain structure of pLIMK1$_{CAT}^{D460N}$ (reported here PDB ID: 5HVJ) and a 2.8 Å structure of cofilin (PDB ID: 4BEX)(Klejnot et al., 2013). Two copies of pLIMK1$_{CAT}^{D460N}$ were found in the asymmetric unit yielding a final translation Z-score of 19.1. This solution was then used to find two copies of cofilin per asymmetric yielding a final translation Z-score of 12.3. Following data treatment with Zanuda (Lebedev and Isupov, 2014) and a first round of refinement using Refmac5 (Murshudov et al., 2011) R/R_{free} were 31.4%/39.3%. Multiple rounds of model building and refinement were carried out using Phenix (Adams et al., 2010) and Coot (Emsley et al., 2010). During these rounds of refinement NCS was turned on and both copies of LIMK1 were built with an AMP-PNP molecule in the catalytic cleft and both copies of cofilin were unphosphorylated. One LIMK1:cofilin heterodimer adequately satisfied the electron density around the catalytic cleft including the *γ*-phosphate of AMP-PNP. In contrast, the second copy displayed clear negative difference density where *γ*-phosphate was built and clear and strong positive difference density immediately adjacent to the hydroxyl group of cofilin Ser3. To satisfy the electron density in this heterodimer we removed the *γ*-phosphate from AMP-PNP to leave AMP-PN and we added a phosphoryl group to Ser3. The resulting model was refined in Phenix in the absence of NCS and resulted in a better model fit to the electron density maps. We skeptically probed this post-catalysis heterodimer with extensive testing of refinement outcomes for multiple conformations of a pre-catalysis model,

but found that in no cases could a pre-catalysis model satisfy the electron density. We further validated the pre- and post-catalysis heterodimer model by consulting simulated annealing omit maps, and found good agreement. We therefore concluded that the electron density supports a model where one heterodimer has undergone phosphotransfer while the other has not. The final R/R_{free} values for the refined structure are 27.3% and 31.0% respectively. The final structure has good geometry, with the Ramachandran statistics showing all residues in favored or allowed conformations. The structure is deposited in the protein data bank under accession code 5HVK.

Kinase Assay

Cofilin phosphorylation

pLIMK1$_{CAT}$ purified as described above was mixed with purified full-length cofilin at a final concentration of 100 nM pLIMK1$_{CAT}$ to 2 μM cofilin in a final volume of 25 μl. The incubation mixture contained 20 mM Tris, pH 7.4, 150 mM NaCl, 5 mM $MgCl_2$, 5 mM $MnCl_2$, 50 μM ATP, 1 mM DTT, 0.1 μCi/ml ^{33}P-ATP and reactions were carried out at 30 °C for 10 minutes. Reactions were quenched by addition of 1 mM EDTA containing 1X SDS-loading buffer and resolved by SDS-PAGE on a 15% polyacrylamide gel. Dried gels are subjected to autoradiography and the level of phosphorylated cofilin is evaluated on a Bio-Rad Molecular Imager Fx system using Quantity One 1D Analysis software (Life Sciences Research).

LIMK1 auto-phosphorylation

Purified LIMK1$_{CAT}$ (WT, M516S and DD549/551KK mutants) was reacted in an incubation mixture that contained 100 nM LIMK1$_{CAT}$, 20 mM Tris, pH 7.4, 150 mM NaCl, 5 mM $MgCl_2$, 5 mM $MnCl_2$, 50 μm ATP, 1 mM DTT, and 0.1 μCi/ml ^{33}P-ATP. Reactions were carried out at 30 °C for 10 minutes and were quenched by addition of 1 mM EDTA containing SDS-loading buffer.

Samples were analyzed by SDS-PAGE and the level of autophosphorylated $LIMK1_{CAT}$ was evaluated on a Bio-Rad Molecular Imager Fx Imaging system using Quantity One software.

Phosphorylation of cofilin in mammalian cells

N-terminally His_6-tagged cofilin DNA (WT, M115A, S119A, K112D) was subcloned into the pCDNA 3.0 mammalian expression vector (Invitrogen). HEK293T cells were plated to 90% confluency in 6-well plates (diameter 3 cm) and transfected with 1 µg cofilin DNA using lipofectamine 2000 reagent (Invitrogen). 36 hours post-transfection, cells were harvested, washed 1X with PBS and lysed in PBS supplemented with 1% Triton. After centrifugation, the supernatants were analyzed by SDS-PAGE and transferred to a nitrocellulose membrane. Membranes were probed with either rabbit anti-phosphocofilin (Ser3) (Cell Signaling, 1:3000 dilution) or mouse anti-His-tag (Sigma, 1:4000) primary antibodies followed by secondary anti-rabbit (LiCor, 1:5000) or anti-mouse (LiCor, 1:3000) IR Dye800 antibodies. Samples were evaluated using a LiCor Odyssey Imaging system.

Yeast growth assays

The vector for constitutive expression of N-terminally hexahistidine-tagged human cofilin-1 in yeast was made by PCR-based cloning into the BamHI and NotI sites of the high copy number plasmid pRS423-GPD, which mediates constitutive expression from the strong glyceraldehyde 3-phosphate dehydrogenase (*TDH3*) promoter. N-terminally FLAG epitope-tagged $LIMK1_{CAT}$ was cloned into the galactose-inducible expression vector pRS416-GAL in between its BamHI and XhoI sites. All point mutants were prepared by QuikChange mutagenesis and verified by sequencing through the entire open reading frame. The temperature sensitive cof1 strain (*cof1-5*) and its otherwise isogenic WT strain were obtained from David Drubin's laboratory (Lappalainen et al., 1997). Yeast doubly transformed with cofilin and $LIMK1_{CAT}$ expressing plasmids or the corresponding empty vectors were grown overnight at 25 °C in synthetic

complete media lacking histidine and uracil (SC-His-Ura) containing 2% glucose. The following day, cultures were diluted into SC-His-Ura containing 2% raffinose and grown overnight to mid-log phase. Serial 5-fold dilutions (starting OD = 0.5) were spotted onto SC-His-Ura agar plates containing either 2% glucose or 2% raffinose/1% galactose, and plates were incubated at either 25 or 37 ºC until colonies were visible in the highest dilution of the WT strain.

SUPPLEMENTAL REFERENCES

Adams, P.D., Afonine, P.V., Bunkoczi, G., Chen, V.B., Davis, I.W., Echols, N., Headd, J.J., Hung, L.W., Kapral, G.J., Grosse-Kunstleve, R.W.*, et al.* (2010). PHENIX: a comprehensive Python-based system for macromolecular structure solution. Acta Crystallogr D Biol Crystallogr *66*, 213-221.

Blanchoin, L., and Pollard, T.D. (1998). Interaction of actin monomers with Acanthamoeba actophorin (ADF/cofilin) and profilin. J Biol Chem *273*, 25106-25111.

Brown, N.R., Noble, M.E., Endicott, J.A., and Johnson, L.N. (1999). The structural basis for specificity of substrate and recruitment peptides for cyclin-dependent kinases. Nat Cell Biol *1*, 438-443.

Dar, A.C., Dever, T.E., and Sicheri, F. (2005). Higher-order substrate recognition of eIF2alpha by the RNA-dependent protein kinase PKR. Cell *122*, 887-900.

Emsley, P., Lohkamp, B., Scott, W.G., and Cowtan, K. (2010). Features and development of Coot. Acta Crystallogr D Biol Crystallogr *66*, 486-501.

Fedorov, A.A., Lappalainen, P., Fedorov, E.V., Drubin, D.G., and Almo, S.C. (1997). Structure determination of yeast cofilin. Nat Struct Biol *4*, 366-369.

Goodwin, N.C., Cianchetta, G., Burgoon, H.A., Healy, J., Mabon, R., Strobel, E.D., Allen, J., Wang, S., Hamman, B.D., and Rawlins, D.B. (2015). Discovery of a Type III Inhibitor of LIM Kinase 2 That Binds in a DFG-Out Conformation. ACS medicinal chemistry letters *6*, 53-57.

Ha, B.H., Davis, M.J., Chen, C., Lou, H.J., Gao, J., Zhang, R., Krauthammer, M., Halaban, R., Schlessinger, J., Turk, B.E.*, et al.* (2012). Type II p21-activated kinases (PAKs) are regulated by an autoinhibitory pseudosubstrate. Proc Natl Acad Sci U S A *109*, 16107-16112.

Hubbard, S.R. (1997). Crystal structure of the activated insulin receptor tyrosine kinase in complex with peptide substrate and ATP analog. Embo J *16*, 5572-5581.

Klejnot, M., Gabrielsen, M., Cameron, J., Mleczak, A., Talapatra, S.K., Kozielski, F., Pannifer, A., and Olson, M.F. (2013). Analysis of the human cofilin 1 structure reveals conformational changes required for actin binding. Acta Crystallogr D Biol Crystallogr *69*, 1780-1788.

Lappalainen, P., Fedorov, E.V., Fedorov, A.A., Almo, S.C., and Drubin, D.G. (1997). Essential functions and actin-binding surfaces of yeast cofilin revealed by systematic mutagenesis. EMBO J *16*, 5520-5530.

Laskowski, R.A. (2009). PDBsum new things. Nucleic Acids Res *37*, D355-359.

Lebedev, A.A., and Isupov, M.N. (2014). Space-group and origin ambiguity in macromolecular structures with pseudo-symmetry and its treatment with the program Zanuda. Acta Crystallogr D Biol Crystallogr *70*, 2430-2443.

Levinson, N.M., Seeliger, M.A., Cole, P.A., and Kuriyan, J. (2008). Structural basis for the recognition of c-Src by its inactivator Csk. Cell *134*, 124-134.

McCoy, A.J. (2007). Solving structures of protein complexes by molecular replacement with Phaser. Acta Crystallogr D Biol Crystallogr *63*, 32-41.

McNicholas, S., Potterton, E., Wilson, K.S., and Noble, M.E. (2011). Presenting your structures: the CCP4mg molecular-graphics software. Acta Crystallogr D Biol Crystallogr *67*, 386-394.

Murshudov, G.N., Skubak, P., Lebedev, A.A., Pannu, N.S., Steiner, R.A., Nicholls, R.A., Winn, M.D., Long, F., and Vagin, A.A. (2011). REFMAC5 for the refinement of macromolecular crystal structures. Acta Crystallogr D Biol Crystallogr *67*, 355-367.

Otwinowski, Z., and Minor, W. (1997). Processing of X-ray diffraction data collected in oscillation mode. In Methods in Enzymology, C.W. Carter, and R.M. Sweet, eds. (San Diego: Academic Press (New York)), pp. 307-326.

Sievers, F., Wilm, A., Dineen, D., Gibson, T.J., Karplus, K., Li, W., Lopez, R., McWilliam, H., Remmert, M., Soding, J.*, et al.* (2011). Fast, scalable generation of high-quality protein multiple sequence alignments using Clustal Omega. Mol Syst Biol *7*, 539.

Xie, T., Peng, W., Yan, C., Wu, J., Gong, X., and Shi, Y. (2013). Structural insights into RIP3-mediated necroptotic signaling. Cell reports *5*, 70-78.

Zheng, J., Trafny, E.A., Knighton, D.R., Xuong, N.H., Taylor, S.S., Ten Eyck, L.F., and Sowadski, J.M. (1993). 2.2 A refined crystal structure of the catalytic subunit of cAMP-dependent protein kinase complexed with MnATP and a peptide inhibitor. Acta Crystallogr D Biol Crystallogr *49*, 362-365.